Please cite as:

J Am Soc Mass Spectrom. 2014 Jun;25(6):906-17. doi: 10.1007/s13361-014-0874-3.

Boundaries of mass resolution in native mass spectrometry.

Lössl P, Snijder J, Heck AJ.

Boundaries of Mass Resolution in Native Mass Spectrometry

Running title: Mass Resolution in Native MS

Key words: Mass resolution, Native mass spectrometry, Desolvation, Adduct formation

Philip Lössl[1,2], Joost Snijder[1,2] and Albert J.R. Heck[1,2*]

[1] Biomolecular Mass Spectrometry and Proteomics. Bijvoet Centre for Biomolecular Research and Utrecht Institute for Pharmaceutical Sciences, University of Utrecht, Padualaan 8, 3584 CH, Utrecht, The Netherlands

[2] Netherlands Proteomics Center, Padualaan 8, 3584 CH, Utrecht, The Netherlands

*Address reprint requests to Albert Heck, Kruytgebouw Room O603, Padualaan 8, 3584 CH Utrecht, The Netherlands, tel: 0031 (0)30 253 6797, fax: 0031 (0)30 253 6919, email: a.j.r.heck@uu.nl

Abstract

Over the last two decades native mass spectrometry (MS) has emerged as a valuable tool to study intact proteins and non-covalent protein complexes. Studied experimental systems range from small-molecule (drug)–protein interactions, to nanomachineries such as the proteasome and ribosome, to even virus assembly. In native MS, ions attain high *m/z* values, requiring special mass analyzers for their detection. Depending on the particular mass analyzer used, instrumental mass resolution does often decrease at higher *m/z* but can still be above a couple of thousand at *m/z* 5,000. However, the mass resolving power obtained on charge states of protein complexes in this *m/z* region is experimentally found to remain well below the inherent instrument resolution of the mass analyzers employed. Here, we inquire into reasons for this discrepancy and ask how native MS would benefit from higher instrumental mass resolution. To answer this question, we discuss advantages and shortcomings of mass analyzers used to study intact biomolecules and biomolecular complexes in their native state and we review which other factors determine mass resolving power in native MS analyses. Recent examples from the literature are given to illustrate the current status and limitations.

Introduction

The mass spectrometric analysis of biomolecules and in particular peptides and proteins is an ongoing success story. It is beyond debate that matrix-assisted laser desorption/ionization (MALDI) [1, 2] and electrospray ionization (ESI) [3] were the crucial inventions to facilitate the development of biomolecular MS from a niche application to today's versatile analytical tool. Beyond that, the evolution of spectroscopic techniques is often described as a "history of resolution" [4]. Indeed, one crucial factor for further progress of protein MS is the continuous improvement of mass spectrometers in terms of resolving power.

Considering the somewhat inconsistent use of terms like 'resolution' and 'resolving power' in the literature, we first describe the definitions of these terms. According to the IUPAC nomenclature, *resolution in mass spectrometry* (R) is defined as $m/\Delta m$ with m being the mass of a singly charged ion in the mass spectrum and Δm being the peak width at a defined fraction of its maximum height (peak width definition) [5], usually taken at 50% (**f**ull **w**idth at **h**alf **m**aximum height, FWHM). Alternatively, Δm may be described as the mass difference of two equally intense peaks so that the valley between them is $\leq$ 10% of their apical intensity (10% valley definition). In contrast, *resolving power in mass spectrometry* has to be defined for at least two points on the peak by expressing the peak width as a function of mass. Confusion arises from the fact that IUPAC separately defines *mass resolving power in mass*

spectrometry in a way similar to the 10% valley definition [5]. Additionally, resolution and resolving power were defined conversely elsewhere [4, 6]. In compliance with the IUPAC recommendations 2013 [7], we adopt here the FWHM peak width definition of resolution.

Nowadays, ultrahigh resolution MS (arbitrary taken as R > 100,000) facilitates accurate protein sequencing and quantification. Fourier transform ion cyclotron resonance (FTICR) and Orbitrap mass analyzers are able to resolve isotopic fine structures of peptides and small proteins [8]. For denatured proteins up to 148 kDa baseline isotopic resolution has been reported with these instruments [9, 10]. Also recent developments in TOF technology come within the realm of ultrahigh mass resolution with R ~ 50,000 being reported [11–14].

Next to its eminent role in peptide sequencing and proteomics, MS has evolved as a valuable tool to study structures, interactions and dynamics of protein complexes [15–17]. Protein assemblies can be ionized under non-denaturing conditions to retain aspects of tertiary and quarternary structures in the gas phase (native MS). This permits the detection of stoichiometries, ligand binding and transient interactions. However, resolutions on individual charge states obtained with native MS are in general much lower than the inherent mass resolution of the used mass analyzers. Yet, native MS has been proven to be a powerful method enabling the analysis of MDa protein complexes, the investigation of subunit arrangement and exchange within non-covalent assemblies as well as the identification of post-translational modifications (PTMs) and ligand binding with great mass accuracy [18–25].

Tackling these problems necessitates different degrees of resolving power. Molecular weight determination depends on the resolution of consecutive charge states which is feasible for protein complexes up to 20 MDa [22]. The determined mass of a protein can, however, be influenced by experimental artifacts such as non-covalently bound buffer or salt molecules and will thus differ from the theoretical molecular weight. While this does not pose a problem for rather uniform assemblies, it complicates the analysis of more complex subunit compositions [26]. The upper mass limit for PTM identification is furthermore substantially lower than for charge state separation since PTMs cause smaller mass shifts. Moreover, some questions are fundamentally elusive to one-dimensional native MS strategies. Defined oligomeric states of polydisperse proteins, such as α-crystallins, cannot be determined in this way as the charge state distributions of the different oligomers largely overlap. Additional tandem MS experiments [27] or complementary biophysical techniques [28] are needed to study population and architecture of the constituent α-crystallin species. Required resolution and its boundaries are therefore largely dependent on the scientific questions at hand.

Here we review resolution limits in the high *m/z* range typical for native MS and evaluate how much resolution we actually need to study different aspects of proteins in their native state. To address this issue, we will briefly compare mass analyzers used for native MS and discuss complementary determinants of the experimentally acquired mass resolution, such as the natural isotope distribution, incomplete desolvation, small molecule and salt adducts as well as detector characteristics. Examples from recent research will be given to elucidate shortcomings imposed by resolution limits and ways to overcome them.

Characteristics of Mass Analyzers Used in Native MS

The high *m/z* regime in which native MS studies are conducted requires mass spectrometers that are specifically dedicated to the analysis of large intact proteins. Albeit such instruments are now commercially available, they are often additionally in-house modified to improve analyte transmission and sensitivity at high *m/z* [29–34].

Up to now most native MS studies have been performed on instruments equipped with a time-of-flight (TOF) analyzer. The popularity of TOF tubes for high-mass analysis is largely due to their wide mass range (only limited by decreasing detector sensitivity [35]) and the fact that there is only a very shallow decline in mass resolution with increasing *m/z*. Likewise, acquisition time does not affect resolution but longer detection will increase the dynamic range [36]. Mass resolution is therefore not impaired by low signal intensity. Signal-to-noise ratios will however increase when individual scans are summed up. Provided that a sample is electrosprayed long enough, even low-abundant species will finally appear as well-resolved peaks. This advantage comes with the drawback of almost complete detection of the chemical background which ultimately limits signal-to-noise ratio and dynamic range [36].

TOF analyzers are often combined with a quadrupole (Q) mass filter to facilitate precursor selection for tandem MS experiments [29, 30]. Hybrid QTOF platforms, with RF generators dedicated for native MS, allow selection of precursor ions up to *m/z* 32,000 [30] and their subsequent collision-induced dissociation (CID), facilitating subunit removal or even fragmentation to b- and y-ions, that may be used for protein identification [37]. Moreover, QTOF instruments coupled to a traveling-wave ion mobility cell add a further analytical dimension to native MS experiments [38]. QTOF tandem mass spectrometry is thus able to provide information about assembly, stoichiometry and, if combined with ion mobility separation, also the shape of a protein complex, making it a very versatile tool to study the architecture of non-covalent assemblies. Subjects as diverse as the subunit composition of the RNA-targeting TtCMr complex [21], the analysis of the 18 MDa viral capsid of the bacteriophage HK97 [22] or

the interaction of carbohydrates with the cholera toxin B subunit homopentamer [18] have been addressed successfully by TOF or QTOF MS (Figure 1). Another intriguing example for the power of this method was recently given by Marcoux *et al.*, who investigated the binding of small molecules to the 140 kDa membrane-embedded transporter P-glycoprotein (P-gp) [19]. Using the previously reported approach of electrospraying intact membrane protein complexes from detergent-containing solutions [39], the authors were able to monitor six binding states of anionic phospholipids, differing by 700-800 Da (Figure 1C), as well as complex formation with cyclic peptide drugs such as cyclosporin A. By means of ion mobility spectrometry, it was furthermore possible to identify two P-gp conformations, the equilibrium of which was shifted by concomitant binding of nucleotides, lipids and drugs but not by individual binding events of these molecules [19]. Native MS thus has proven to be a valuable addition to the biochemical toolbox for investigating ligand binding and allostery.

Although less frequently used for this purpose, FTICR platforms are also appropriate to investigate intact proteins and protein assemblies. Furthermore, an Orbitrap Exactive Plus with an extended mass range (EMR) suitable for native MS applications has been introduced in 2012 [33]. When used for the analysis of intact proteins, the performance of FTICR cells and (to a lower extent) also Orbitraps can be affected by space-charge effects, as a high number of charges per analyte is introduced in the mass analyzer [40, 41]. However, it may also be argued that these multiply charged analytes induce larger image currents allowing even single molecule detection [33]. Furthermore, in particular in the FTICR trap, the used magnetic field induces next to the cyclotron motion also high-magnitude magnetron motions especially for high mass ions, limiting their trapping efficiency [42, 43]. Further restraints are imposed by the Fourier transform (FT)-based detection method. Resolved isotopes generate beat patterns within the transients recorded in FTMS. The increased number of isotopes for high-mass ions results in narrower beats with longer in-between time intervals without significant signal, consequently leading to a signal decrease [44]. Moreover, acquiring high resolution in FTICR and Orbitrap MS requires sufficiently long measurement of the image current transients, which may go up to seconds and even minutes to obtain isotope resolution for a large protein. This requires stable oscillations of the analyte ions but field imperfections, space-charge effects and collisions with background gas ions contribute to a rapid decay [40, 45]. In fact, Makarov and Denisov deduced that fragmenting and non-fragmenting collisions are the main reasons for ion loss within the Orbitrap [46]. As big molecular ions, due to their large collision cross sections, are very likely to collide with residual gas molecules, it is not trivial to generate stable long transients for large intact proteins. However, if ion transients can be recorded long enough,

Orbitrap and FTICR platforms are capable of higher resolution than TOF instruments. Moreover, chemical background is clearly reduced in FTMS since background ions need to oscillate in stable transients to be detected by the FT algorithm [36].

Hybrid QFTICR platforms facilitate precursor ion selection in the quadrupole with an upper selection limit of *m/z* 6,000 in accordance with previous native MS studies [47]. Thus, these mass spectrometers are basically usable in a similar way as QTOFs. Additionally, they provide a wide range of fragmentation techniques apart from CID, e. g. electron capture dissociation (ECD), blackbody infrared dissociation (BIRD) and infrared multiphoton dissociation (IRMPD) [34, 47]. Especially ECD was shown to be useful to obtain sequence information of intact proteins in a top-down approach [47, 48]. In the low mass range (*m/z* < 2.,000) isotopically resolved top-down MSMS spectra have been obtained with QTOF as well as QFTICR instruments [48, 49]. However, FTMS-based mass spectrometers may offer a greater potential for obtaining isotope resolution also for fragment ions in higher *m/z* regions. Using an Orbitrap Q-Exactive with extended mass range, pyruvate kinase fragment ions with a maximum mass of 11,000 Da could be isotopically resolved by native top-down MS [50]. This recently introduced mass spectrometer is equipped with a dual ion funnel device, enabling in-source desolvation of the analyte, and a quadrupole mass filter, that allows precursor selection up to 20,000 *m/z*. Currently, protein ions can only be fragmented via higher-energy collisional dissociation (HCD). However, owing to the high resolving power of the Orbitrap, this instrument can potentially open up new avenues in native MS analysis. The Orbitrap Exactive Plus EMR, first reported in 2012 [33], was already proven to be an important advance for the field since it is able to resolve small mass shifts even in complex spectra enabling, for example, the identification and quantification of complex glycosylation profiles of antibody mixtures [23, 51].

Boundaries of the Apparent Mass Resolution in the High Mass Range

In spite of the accomplishments made possible by all these instruments there is still plenty room for improvement. Most notably, the inherent mass resolution of each mass analyzer (R_{max}), i. e. the maximum instrument mass resolution, is found to deviate substantially from that obtained experimentally on native proteins (R_{nat}). This is exemplified by a comparison of mass resolutions reported at *m/z* 5,000–6,000, which corresponds to the detection range of ions of a 150 kDa globular soluble protein in native MS. Typically, R_{max} is experimentally probed by measuring very large monoisotopic CsI clusters. When these experiments are conducted under conditions also used

for native MS, R_{max} at *m/z* 5,000–6,000 reaches up to 7,000 for TOF [30] and 25,000 for Orbitrap [33]. In contrast, the highest R_{nat} achieved with these same mass analyzers is reduced to much lower values, ranging from 1,500 (on a TOF) [52] to about 5,500 (on an Orbitrap) [23]. Using a FTICR mass spectrometer equipped with a distinctive ParaCell [53, 54], Li *et al.* were able to obtain isotope resolution on native 158 kDa tetrameric aldolase ($R \approx$ 520,000) [55]. Here, we adopt a more conservative estimation of R_{max} = 40,000 for most currently used FTICR analyzers.

We now want to illustrate the performance potential at high *m/z* values when R_{max} could be fully exploited. For the following comparisons, instrument-inherent disparities between analyzing CsI clusters and native proteins (such as transmission properties [31, 56, 57], space-charge effects [40] or ion dispersion [58, 59]), that influence the obtainable resolution, are disregarded. The first prerequisite of accurate and precise mass determination of intact proteins in native MS is to resolve their consecutive charge states, such that the molecular weight can be calculated from the obtained *m/z* values [60]. In Figure 2, we plotted both R_{max} of the different analyzers and the resolution required for the separation of consecutive charge states as a function of *m/z*. For each given mass analyzer, the point where these curves intersect represents the *m/z* at which consecutive charge states are separated at half height. Each analyzer should evidently be able to discriminate between consecutive charge states up to $m/z > 50{,}000$. This covers the entire mass range of FTICR cells and Orbitraps. TOF resolution even seems to impose limits only above *m/z* 245,000, which is beyond the scope of most detectors used in native MS instruments but would also correspond to extremely large protein complexes (> 500 MDa). Since R_{nat} of TOF and QTOF mass spectrometers is, however, significantly lower than their theoretical R_{max}, charge state separation of protein ions is restricted to $m/z \leq 52{,}000$ [22]. Next, we want to discuss reasons for this discrepancy between R_{nat} and R_{max}.

Native MS Cannot Resolve Binding of Salt and Buffer Molecules to Proteins Larger Than 65 kDa

Apart from the maximum instrument mass resolution, there are additional, mass analyzer-independent factors that influence R_{nat}, in particular incomplete desolvation of the analyte and/or unwanted association of buffer or salt molecules as well as the width of the analyte's natural isotope distribution. To illustrate these factors, we added two further resolution-versus-*m/z* plots to Figure 2:

The red curve represents the theoretical maximum resolution obtainable for a native globular protein, as it is defined by the width of its natural occurring isotope envelope [22]. The orange curve corresponds to the minimum resolution that is needed to resolve binding of one Na^+ instead of a proton to a multiply charged protein. We take this example as it is one of the most common features disturbing mass resolving power in native MS, caused by residual salt in the buffer that leads to parallel generation of $[M+nH]^{n+}$ and $[M+(n-1)H+Na]^{n+}$ ions.

By comparing these curves, we can estimate at any given *m/z* whether it would be fundamentally feasible to resolve the sodium-bound protein ion from the corresponding molecular ion. The red and orange curves intersect at *m/z* 4,000 (corresponding to a protein mass of ~ 65 kDa in native MS), clarifying that it is intrinsically impossible to separate unmodified native proteins and mono-sodium-adduct species at half-maximum height beyond this limit. Notably, the inherent resolving power of all three commonly used mass analyzers does not impose any practical limitations since R_{max} of each analyzer would allow to resolve Na^+ binding events up to *m/z* values higher than 4,000. Consequently, regardless of the maximum instrument mass resolution, the presence of adduct-bound protein ions results in many closely spaced signals that merge into a single broad peak contributing to the relatively low R_{nat} that is usually obtained in native MS experiments.

One could hypothesize that the limitations imposed by the dimensions of the isotope envelope could be overcome by obtaining isotope resolution. The work of Li *et al*. illustrates that resolving isotope patterns indeed diminishes the discrepancy between R_{nat} and R_{max} because R_{nat} can now be determined for a single isotope peak rather than for a protein ion peak, that consists of all its isotopes. Though, it is still impossible to separate the isotope distributions of unmodified and adduct-bound species [55]. This is also illustrated in Figure 3, where we simulate the 26+ charge state of a 150 kDa "Averagine" protein (1,350 Averagine residues [61]) in its unmodified, ammonium-bound and sodium-bound form. Each species is simulated assuming baseline isotope resolution. However, due to their small *m/z* differences they are not distinguishable in the summed spectrum. Instead, the interference of the individual isotope distributions results in a distorted isotope envelope that has lost its typical bell shape. In this simulation, we only take two possible adducts in consideration but in reality more small molecule and salt adducts are likely to be co-occurring. Interpretation of isotope patterns therefore becomes increasingly difficult and peak assignment has to be performed with dedicated analysis software [62, 63] or by comparing simulated and experimental isotope distributions with a least chi-square test [9, 61, 64]. Furthermore, peaks in isotope-resolved spectra are usually of lower maximum intensity, as the signal spreads over all isotopes, and also present a challenge to the FT detection

algorithm. Although resolving isotope patterns of large native proteins or protein complexes remains an appealing challenge from a technical point of view, it will neither improve the accuracy of mass determination (compared to the theoretical 'bare' protein ions) nor enhance separation of adduct-bound species in the high *m/z* regime. Despite this limited gain of information with regard to mass accuracy and effective resolution of high *m/z* species, it should be noted that isotope-resolved spectra do offer additional information for charge-state assignments. This is of particular interest for peak assignment strategies in top-down native MS analyses of non-covalent protein complexes [48–50, 55, 65].

Incomplete Removal of Unwanted Adducts Is the Major Mass Resolution-Limiting Factor in Native MS

As reviewed above, the apparent mass resolution observed for proteins in native MS is predominantly influenced by three factors: I. Inherent mass resolution of the mass analyzer, II. Width of the natural isotope distribution of the analyte ion and III. Efficiency of desolvation in the ESI process, i. e. adduct removal from the analyte.

In Figure 4A, we illustrate the impact of these aspects, taking the 71+ charge state of the 800 kDa bacterial chaperonin GroEL at *m/z* ~ 11,000. The signal of this protein ion was measured on a QTOF and an Orbitrap instrument, both operating at R_{max} = 5,000, and additionally simulated for different instrumental R_{max}. For both experimental and simulated spectra we also calculated the apparent mass resolution R_{nat} by determining the FWHM of each peak. In Figure 4B, R_{nat} of the simulated GroEL peaks is plotted against the respective R_{max} values that were originally assumed for the simulations. This plot makes clear that, in the range of low inherent mass analyzer resolutions, R_{nat} greatly benefits from a higher R_{max}. This positive correlation becomes weaker as R_{nat} approximates the ultimate resolution limit that is given by the width of the natural isotope envelope. Considering the inherent resolutions of current mass analyzers, further R_{max} enhancements would only have a modest impact on the apparent mass resolution obtained with native proteins. In reality, this small effect would be clearly overruled by the much larger impact of incomplete desolvation. This becomes apparent by comparing the Orbitrap and the QTOF spectra with the mass spectrum that was simulated at R_{max} = 5,000. Although the inherent instrument resolution is the same in each case, we encountered substantial differences for the apparent resolution: R_{nat} in the simulation, where only 'bare' GroEL ions are considered, is two–three times higher than in the experimental QTOF or Orbitrap spectra. This is largely due to the fact that the experimental peaks represent, next to the 'bare' ions, also additional species

with buffer or salt molecules attached. Hence, R_{nat} is reduced mainly because of incomplete desolvation. At the same time, the apparent resolution obtained with the Orbitrap is almost twice as high (2,400) as with the QTOF (1,300). Since both mass spectrometers were operated at equal instrumental R_{max} this difference is most likely attributable to more efficient desolvation in the Orbitrap. As we will discuss later on, most adducts are stripped off in the source region and the collision cell of an instrument. The design of both these parts within the Orbitrap EMR is very distinct from that on the existing QTOF platforms. Therefore, a main reason for its superior resolving power in native MS may be an advantageous source and collision cell architecture facilitating higher desolvation efficiency.

Our simulations and measurements thus affirm the previous statement made by Zhang *et al.* [65], that the apparent resolution and the offset between calculated and experimental protein ion masses in native MS are more affected by the efficiency of adduct elimination and analyte desolvation than by the inherent mass resolution of the current analyzers.

Most importantly, elimination of small molecule adducts can be enhanced by collisional activation of protein ions [34, 37, 66]. In native MS, this "cleaning-up" is often performed in a collision cell, that is filled with neutral inert gas atoms or molecules. Collisions with the background gas raise the internal energy of the protein ions, leading to a progressive loss of bound adducts [67]. However, ion mobility studies have elucidated that the CID process may, depending on the extent of activation, enforce structural rearrangements, either compaction and/or subunit unfolding, dissociation and eventually fragmentation [68]. Native MS experiments are often performed with acceleration voltages that only just prevent subunit dissociation [69] but under such conditions conformational changes within the analyzed biomolecular complex may already occur [70]. Whereas structural changes do not compromise molecular weight or stoichiometry determination they will interfere with any analysis aiming for information on the gas phase structure of non-covalent assemblies. In these cases careful weighing of the benefit of improved desolvation against the danger of structural deterioration is required.

Sun *et al.* systematically investigated several factors influencing the association of small molecules during the ESI process of proteins. Experiments were carried out with basic and acidic molecules that could associate with three model proteins. These results suggest that the binding process is purely random and therefore not influenced by inherent protein characteristics such as size and structure. The nature of the protein ions does, however, affect the kinetic stability of these protein–small molecule interactions making them differentially resistant to dissociation in the ion source [71].

For the analysis of larger proteins by native MS it is almost inevitable that some undesired adducts remain attached. Generally, desolvation efficiency decreases with increasing protein complex size, causing the apparent resolution to decay irrespective of the inherent mass analyzer characteristics. This was recently illustrated in our mass analysis of intact capsids of the bacteriophage HK97 using a QTOF instrument, the resolution of which shows only a very shallow drop-off with increasing *m/z* [22]. This virus assembly has a molecular weight of 18 MDa and was detected at *m/z* ~ 52,000. The apparent mass resolving power was just high enough to separate charge states indicating that the upper mass limit for native MS with these instruments is currently around 20 MDa, when charge state resolution is considered as a prerequisite. However, measuring CsI clusters had already proven that a resolution of several thousands can be reached with TOFs operating even in this very high *m/z* region [22, 30]. In fact, the width of the natural isotope distribution and the inherent instrument resolution would allow baseline separation of charge states but desolvation limits R_{nat} to approximately 200. Notably, the 20 MDa limit described here applies to the requirements of mass determination from a relatively simple spectrum. Substantially higher resolution is needed to identify PTMs or to distinguish between different components in a more complex spectrum.

Attempts to Minimize Resolution-Related Shortcomings

In view of the limitations in apparent resolution there is a constant strive to augment the quality of information that can be obtained from native MS experiments. Prospects for satisfactory removal or separation of adduct-bound species are in general chiefly protein dependent. Accurately determining the molecular weight of unknown assemblies thus requires an estimation of the mass error caused caused by undesired adduct formation. The analysis of non-covalent assemblies of 365-800 kDa revealed that percentage mass increase scales linearly with peak width normalized to *m/z*. In combination with manual charge state assignment this approach was used to determine the masses of the 70S ribosome and its components [26]. Later studies made clear that, in contrast to initial assumptions, the slope of this linear relationship depends on instrument parameters like pressure in the first regions of differential pumping [72]. Consequently, high-confidence mass assignments, enabling the determination of subunit compositions for assemblies as complex as the 70S ribosome, still necessitate thorough instrument-specific calibration with known protein complexes.

Since resolution boundaries mainly arise from incomplete desolvation it seems straightforward to explore novel, non-denaturing buffer substances that are highly volatile to evaporate during the ESI process. These requirements

are quite obvious, yet there are not many matching compounds. So far, almost exclusively aqueous ammonium acetate has been used. Recently, Dyachenko *et al.* introduced a new buffer substance, ethylenediammonium diacetate (EDDA), to study the allosteric regulation of ATP binding to GroEL [73]. The authors used this buffer as ammonium acetate was reported not to be suitable for this analysis since NH_4^+ supports ATP hydrolysis. When samples were sprayed from an EDDA buffer, intact GroEL 14mers carried almost 18 charges less compared to when sprayed from aqueous ammonium acetate. Nonetheless, EDDA clearly improved peak resolution enabling the distinction of the ATP loading states (Figure 5) and their corresponding binding constants on a QTOF platform. The positive effects of EDDA can partially be attributed to the prevention of ATP hydrolysis since mixed ATP/ADP complexes do not complicate the spectra. Though, even in absence of ATP peaks were still better resolved indicating that analyte desolvation is generally more efficient when using EDDA buffer, at least for GroEL [73]. In light of these findings EDDA appears to be a promising alternative to ammonium acetate, allowing higher apparent resolutions to be obtained. However, follow-up studies are necessary to investigate whether the described features are generic and applicable to other protein systems. As the kinetic energy of analyte ions entering the collision cell increases with their charge state, it also has to be examined to which extent the charge-reducing properties of EDDA compromise experiments requiring collision-induced dissociation of non-covalent assemblies.

We already mentioned that, on the instrumental side, desolvation efficiency is greatly affected by the construction of both the source region and the collision cell since most adducts may be stripped off at these stages. Despite the drawbacks of adduct elimination by CID, it is still important to exploit the full potential of this approach. Depending on the object (i. e. protein system) and purpose (e. g. molecular weight determination, PTM identification or stoichiometry assignment) of a native MS study, the available collision energy and hence the degree of analyte desolvation may be insufficient to answer the scientific question. At the same time, studying complex dissociation is not possible if collision energies are too low. Collision energy depends on the acceleration voltage as well as the masses of collision gas molecules and protein ions [66]. Using a heavier collision gas or higher voltages will therefore increase the potential collision energies. Lorenzen *et al.* demonstrated that small modifications of the collision cell and utilization of a heavy collision gas (xenon instead of argon) enhances GroEL dissociation and focuses the ions more effectively [66]. Complementary, Benesch *et al.* investigated the effect of elevated acceleration voltages on Heat Shock Protein 16.5 from *M. jannaschii* (396 kDa). Whereas 200 V were sufficient to dissociate monomeric subunits, even b- and y- fragment ions were observed when the voltage was further increased

[37]. Depending on the gas-phase stability of the protein complex, increased acceleration voltages combined with a heavy collision gas will thus allow better desolvation, subunit dissociation or even top-down acquisition of sequence information.

Limitations of CID-enforced desolvation also arise with respect to accurate tandem MS experiments. Quadrupole-enabled precursor ion selection in QTOF and QFTICR instruments proceeds prior to the analyte "cleaning" in the collision cell. At the selection stage, these ions are consequently less resolved than they appear to be in the TOF mass spectra. This may lead to unwanted co-isolation of adjacent ions from either different species or charge states. A way to account for this problem is to enhance pre-quadrupole desolvation of protein complexes by allowing higher voltages in the source region of the instrument. To illustrate these effects we recorded tandem mass spectra of gp5 capsomers from bacteriophage HK97 on a QTOF platform. The capsomers form a mixture of pentamers and hexamers, the ions of which are close in *m/z* when analyzed with native MS. A well-resolved TOF mass spectrum, acquired at high activation energy, was used to select the base peak of the pentameric complex (Figure 6A). The quadrupole accurately selects ions of this *m/z* as evidenced from a tandem mass spectrum acquired at low collision voltage (Figure 6B). However, incomplete desolvation causes peaks to be shifted in *m/z* at the quadrupole stage. When the selected ions are further desolvated in the collision cell they hence appear at a different *m/z* in the tandem mass spectra clarifying that they actually correspond to different compounds (Figure 6C). For gp5 capsomers, the majority of selected ions are actually hexameric complexes instead of the supposedly selected pentamers. By applying in-source activation, this co-isolation can be prevented and pentamers can be selected at the *m/z* values at which they appear in well-resolved spectra (Figure 6D).

Although proper instrument tuning can substantially improve mass resolution, it is still not trivial to identify small mass changes in large protein assemblies due to ligand binding or truncations. We already mentioned that resolving oligomeric states can be even more problematic since peaks, that are consistent with the n-mer, do, in principle, correspond to any (x_*n)-mer as well (with x and n being natural numbers). It is hence quite difficult to separate oligomers of the same biomolecule, if they are populated in the same *m/z* range. Likewise, poor resolution of one high-abundant oligomer will impair molecular weight determination of all the other species. However, in early native MS studies of amyloid formation, which we will use as an illustrative example, oligomer size was determined solely based on *m/z* [74]. Since oligomerization as well as the other mentioned variations may have a great effect on complex size and/or conformation the, distinction of species will be simplified by ion mobility separation prior to

mass spectrometric analysis (IMMS). Theoretical principles and practical aspects of IMMS have been described in detail elsewhere [38, 75]. Separation by ion mobility spectrometry is based on charge and collision cross sections enabling discrimination of proteins with different shapes regardless of their masses. The separation of Amyloid β (Aβ) oligomers, described by Kloniecki *et al.*, may serve as an example for the substantial advances IMMS has brought about in the field of amyloid research [76]. At *m/z* 2164-2169, overlapping charge state distributions of monomeric, dimeric, trimeric and tetrameric Aβ are present (Figure 7, left panel). Nonetheless, identification of all species is feasible as they carry different numbers of charges and vary in their collision cross sections, resulting in distinct mobilities of the protein ions (Figure 7, right panel). Moreover, two different conformations of the Aβ trimer, compact and extended, are clearly resolved.

Conclusion

In this work we tried to address limiting factors of mass resolving power in native mass spectrometry of large protein assemblies. The answer to the question of how much resolution is needed for native MS depends on what we are aiming for and what we are looking at. Separation of consecutive charge states is sufficient to determine a compound's molecular weight – a condition dictating that we just need R ≈ 200 for a 20 MDa species at *m/z* ~ 52,000. Higher resolution is still required for the identification of PTMs or bound small molecule ligands on ~ 100-800 kDa proteins and protein assemblies. Equally, highly complex spectra will be annotated with greater confidence and more compounds will be identified when peaks are better mass resolved. Due to the natural isotope distribution and the charge states of intact proteins it is however fundamentally impossible to separate species with a different number of adducts bound. Resolving isotope patterns in the high *m/z* range (~ 100–200 kDa) is therefore primarily of academic interest.

Limitations in apparent resolution still prohibit access to the full depth of information contained in the mass spectra, restrain the upper mass limit and reduce the power of tandem MS experiments. These restrictions are not set by currently used mass analyzers but primarily imposed by inefficient desolvation of the analyte and/or mass heterogeneity of the measured molecules. However, instrumentation has remarkably improved over the last decade. Owing to continuous development of methods and hardware a wide variety of problems can now be addressed. Technical developments in native MS are still far away from inertia as exemplified by approaches reviewed in this article such as the development of the Orbitrap instruments with extended mass range, the potential of which we

have only just begun to understand. Hence, the road is paved to further push the limits of mass resolving power in native MS.

Acknowledgements

This work, and in particular PL and AJRH, has been supported by the ManiFold project, grant agreement number 317371, and in part by the PRIME-XS project, Grant Agreement Number 262067, both funded by the European Union 7th Framework Programme. The Netherlands Proteomics Centre, embedded in The Netherlands Genomics Initiative, is acknowledged for funding.

References

1. Tanaka, K., Waki, H., Ido, Y., Akita, S., Yoshida, Y., Yoshida, T., Matsuo, T.: Protein and polymer analyses up to m/z 100 000 by laser ionization time-of-flight mass spectrometry. *Rapid Commun. Mass Spectrom.*, **2**, 151–153 (1988)
2. Karas, M., Bachmann, D., Bahr, U., Hillenkamp, F.: Matrix-assisted ultraviolet laser desorption of non-volatile compounds. *Int. J. Mass Spectrom. Ion Process.*, **78**, 53–68 (1987)
3. Fenn, J.B., Mann, M., Meng, C.K., Wong, S.F., Whitehouse, C.M.: Electrospray ionization for mass spectrometry of large biomolecules. *Science*, **246**, 64–71 (1989)
4. Marshall, A.G., Hendrickson, C.L.: High-resolution mass spectrometers. *Annu. Rev. Anal. Chem.*, **1**, 579–599 (2008)
5. McNaught, A.D., Wilkinson, A.: Compendium of chemical terminology. IUPAC recommendations. 2nd ed. *Blackwell Science*: Oxford (1997)
6. Sparkman, O.D.: Mass spectrometry desk reference. 2nd ed. *Global View Pub.*: Pittsburgh, Pa (2006)
7. Murray, K.K., Boyd, R.K., Eberlin, M.N., Langley, G.J., Li, L., Naito, Y.: Definitions of terms relating to mass spectrometry (IUPAC recommendations 2013). *Pure Appl. Chem.*, **85**, 1515–1609 (2013)
8. Miladinović, S.M., Kozhinov, A.N., Gorshkov, M.V., Tsybin, Y.O.: On the utility of isotopic fine structure mass spectrometry in protein identification. *Anal. Chem.*, **84**, 4042–4051 (2012)
9. Valeja, S.G., Kaiser, N.K., Xian, F., Hendrickson, C.L., Rouse, J.C., Marshall, A.G.: Unit mass baseline resolution for an intact 148 kDa therapeutic monoclonal antibody by Fourier transform ion cyclotron resonance mass spectrometry. *Anal. Chem.*, **83**, 8391–8395 (2011)
10. Shaw, J.B., Brodbelt, J.S.: Extending the isotopically resolved mass range of Orbitrap mass spectrometers. *Anal. Chem.*, **85**, 8313–8318 (2013)
11. Andrews, G.L., Simons, B.L., Young, J.B., Hawkridge, A.M., Muddiman, D.C.: Performance characteristics of a new hybrid quadrupole time-of-flight tandem mass spectrometer (TripleTOF 5600). *Anal. Chem.*, **83**, 5442–5446 (2011)
12. Holčapek, M., Jirásko, R., Lísa, M.: Recent developments in liquid chromatography–mass spectrometry and related techniques. *J. Chromatogr. A*, **1259**, 3–15 (2012)

13. Lee, J., Chen, H., Liu, T., Berkman, C.E., Reilly, Peter T. A.: High resolution time-of-flight mass analysis of the entire range of intact singly-charged proteins. *Anal. Chem.*, **83**, 9406–9412 (2011)

14. Pelander, A., Decker, P., Baessmann, C., Ojanperä, I.: Evaluation of a high resolving power time-of-flight mass spectrometer for drug analysis in terms of resolving power and acquisition rate. *J. Am. Soc. Mass Spectrom.*, **22**, 379–385 (2011)

15. Gordiyenko, Y., Robinson, C.V.: The emerging role of MS in structure elucidation of protein–nucleic acid complexes. *Biochem. Soc. Trans.*, **36**, 723–731 (2008)

16. Heck, A.J.R.: Native mass spectrometry: a bridge between interactomics and structural biology. *Nat. Meth.*, **5**, 927–933 (2008)

17. Sharon, M.: Structural MS pulls its weight. *Science*, **340**, 1059–1060 (2013)

18. Zhang, Y., Deng, L., Kitova, E.N., Klassen, J.S.: Dissociation of multisubunit protein–ligand complexes in the gas phase. Evidence for ligand migration. *J. Am. Soc. Mass Spectrom.*, **24**, 1573–1583 (2013)

19. Marcoux, J., Wang, S.C., Politis, A., Reading, E., Ma, J., Biggin, P.C., Zhou, M., Tao, H., Zhang, Q., Chang, G., Morgner, N., Robinson, C.V.: Mass spectrometry reveals synergistic effects of nucleotides, lipids, and drugs binding to a multidrug resistance efflux pump. *Proc. Natl. Acad. Sci. U.S.A.*, **110**, 9704–9709 (2013)

20. Zhou, M., Sandercock, A.M., Fraser, C.S., Ridlova, G., Stephens, E., Schenauer, M.R., Yokoi-Fong, T., Barsky, D., Leary, J.A., Hershey, J.W., Doudna, J.A., Robinson, C.V.: Mass spectrometry special feature: mass spectrometry reveals modularity and a complete subunit interaction map of the eukaryotic translation factor eIF3. *Proc. Natl. Acad. Sci. U.S.A.*, **105**, 18139–18144 (2008)

21. Staals, R.H., Agari, Y., Maki-Yonekura, S., Zhu, Y., Taylor, D.W., van Duijn, E., Barendregt, A., Vlot, M., Koehorst, J.J., Sakamoto, K., Masuda, A., Dohmae, N., Schaap, P.J., Doudna, J.A., Heck, A.J., Yonekura, K., van der Oost, John, Shinkai, A.: Structure and activity of the RNA-targeting type III-B CRISPR-Cas complex of Thermus thermophilus. *Mol. Cell*, **52**, 135–145 (2013)

22. Snijder, J., Rose, R.J., Veesler, D., Johnson, J.E., Heck, A.J.R.: Studying 18 MDa virus assemblies with native mass spectrometry. *Angew. Chem. Int. Ed.*, **52**, 4020–4023 (2013)

23. Rosati, S., Rose, R.J., Thompson, N.J., van Duijn, E., Damoc, E., Denisov, E., Makarov, A., Heck, A.J.R.: Exploring an Orbitrap analyzer for the characterization of intact antibodies by native mass spectrometry. *Angew. Chem. Int. Ed.*, **51**, 12992–12996 (2012)

24. Videler, H., Ilag, L.L., McKay, A.R., Hanson, C.L., Robinson, C.V.: Mass spectrometry of intact ribosomes. *FEBS Lett.*, **579**, 943–947 (2005)

25. Keetch, C.A., Bromley E.H., McCammon M.G., Wang N., Christodoulou J., Robinson C.V.: L55P transthyretin accelerates subunit exchange and leads to rapid formation of hybrid tetramers. *J. Biol. Chem.*, **280**, 41667–41674 (2005)

26. McKay, A.R., Ruotolo, B.T., Ilag, L.L., Robinson, C.V.: Mass measurements of increased accuracy resolve heterogeneous populations of intact ribosomes. *J. Am. Chem. Soc.*, **128**, 11433–11442 (2006)

27. Aquilina, J.A., Benesch, Justin L P, Bateman, O.A., Slingsby, C., Robinson, C.V.: Polydispersity of a mammalian chaperone: mass spectrometry reveals the population of oligomers in alphaB-crystallin. *Proc. Natl. Acad. Sci. U.S.A.*, **100**, 10611–10616 (2003)

28. Baldwin, A.J., Lioe, H., Hilton, G.R., Baker, L.A., Rubinstein, J.L., Kay, L.E., Benesch, J.L.: The Polydispersity of αB-Crystallin Is Rationalized by an Interconverting Polyhedral Architecture. *Structure*, **19**, 1855–1863 (2011)

29. van den Heuvel, R.H.H., van Duijn, E., Mazon, H., Synowsky, S.A., Lorenzen, K., Versluis, C., Brouns, S.J.J., Langridge, D., van der Oost, J., Hoyes, J., Heck, A.J.R.: Improving the performance of a quadrupole time-of-flight instrument for macromolecular mass spectrometry. *Anal. Chem.*, **78**, 7473–7483 (2006)

30. Sobott, F., Hernández, H., McCammon, M.G., Tito, M.A., Robinson, C.V.: A tandem mass spectrometer for improved transmission and analysis of large macromolecular assemblies. *Anal. Chem.*, **74**, 1402–1407 (2002)

31. Chernushevich, I.V., Thomson, B.A.: Collisional cooling of large ions in electrospray mass spectrometry. *Anal. Chem.*, **76**, 1754–1760 (2004)

32. Kozlovski, V., Donald, L., Collado, V., Spicer, V., Loboda, A., Chernushevich, I., Ens, W., Standing, K.: A TOF mass spectrometer for the study of noncovalent complexes. *Int. J. Mass Spectrom.*, **308**, 118–125 (2011)

33. Rose, R.J., Damoc, E., Denisov, E., Makarov, A., Heck, A.J.R.: High-sensitivity Orbitrap mass analysis of intact macromolecular assemblies. *Nat. Meth.*, **9**, 1084–1086 (2012)

34. Kaiser, N.K., Quinn, J.P., Blakney, G.T., Hendrickson, C.L., Marshall, A.G.: A novel 9.4 Tesla FTICR mass spectrometer with improved sensitivity, mass resolution, and mass range. *J. Am. Soc. Mass Spectrom.*, **22**, 1343–1351 (2011)

35. Chen, X., Westphall, M.S., Smith, L.M.: Mass spectrometric analysis of DNA mixtures: instrumental effects responsible for decreased sensitivity with increasing mass. *Anal. Chem.*, **75**, 5944–5952 (2003)

36. Zubarev, R.A., Makarov, A.: Orbitrap mass spectrometry. *Anal. Chem.*, **85**, 5288–5296 (2013)

37. Benesch, J.L.P., Ruotolo, B.T., Sobott, F., Wildgoose, J., Gilbert, A., Bateman, R., Robinson, C.V.: Quadrupole-time-of-flight mass spectrometer modified for higher-energy dissociation reduces protein assemblies to peptide fragments. *Anal. Chem.*, **81**, 1270–1274 (2009)

38. Uetrecht, C., Rose, R.J., van Duijn, E., Lorenzen, K., Heck, A.J.R.: Ion mobility mass spectrometry of proteins and protein assemblies. *Chem. Soc. Rev.*, **39**, 1633–1655 (2010)

39. Barrera, N.P., Di Bartolo, N., Booth, P.J., Robinson, C.V.: Micelles protect membrane complexes from solution to vacuum. *Science*, **321**, 243–246 (2008)

40. Perry, R.H., Cooks, R.G., Noll, R.J.: Orbitrap mass spectrometry: instrumentation, ion motion and applications. *Mass Spectrom. Rev.*, **27**, 661–699 (2008)

41. Easterling, M.L., Mize, T.H., Amster, I.J.: Routine part-per-million mass accuracy for high-mass ions: space-charge effects in MALDI FT-ICR. *Anal. Chem.*, **71**, 624–632 (1999)

42. Ledford, E.B., Rempel, D.L., Gross, M.L.: Space charge effects in Fourier transform mass spectrometry. II. Mass calibration. *Anal. Chem.*, **56**, 2744–2748 (1984)

43. Schweikhard, L., Ziegler, J., Bopp, H., Lützenkirchen, K.: The trapping condition and a new instability of the ion motion in the ion cyclotron resonance trap. *Int. J. Mass Spectrom. Ion Process.*, **141**, 77–90 (1995)

44. Hofstadler, S.A., Bruce, J.E., Rockwood, A.L., Anderson, G.A., Winger, B.E., Smith, R.D.: Isotopic beat patterns in Fourier transform ion cyclotron resonance mass spectrometry: implications for high resolution mass measurements of large biopolymers. *Int. J. Mass Spectrom. Ion Process.*, **132**, 109–127 (1994)

45. Scigelova, M., Hornshaw, M., Giannakopulos, A., Makarov, A.: Fourier transform mass spectrometry. *Mol. Cell. Proteomics*, **10**, 1–19 (2011)

46. Makarov, A., Denisov, E.: Dynamics of ions of intact proteins in the Orbitrap mass analyzer. *J. Am. Soc. Mass Spectrom.*, **20**, 1486–1495 (2009)

47. Zhang, H., Cui, W., Wen, J., Blankenship, R.E., Gross, M.L.: Native electrospray and electron-capture dissociation FTICR mass spectrometry for top-down studies of protein assemblies. *Anal. Chem.*, **83**, 5598–5606 (2011)

48. Zhang, H., Cui, W., Wen, J., Blankenship, R.E., Gross, M.L.: Native electrospray and electron-capture dissociation in FTICR mass spectrometry provide top-down sequencing of a protein component in an intact protein assembly. *J. Am. Soc. Mass Spectrom.*, **21**, 1966–1968 (2010)

49. Lermyte, F., Konijnenberg, A., Williams, J.P., Brown, J.M., Valkenborg, D., Sobott, F.: ETD Allows for Native Surface Mapping of a 150 kDa Noncovalent Complex on a Commercial Q-TWIMS-TOF Instrument. *J. Am. Soc. Mass Spectrom.* (2014)

50. Belov, M.E., Damoc, E., Denisov, E., Compton, P.D., Horning, S., Makarov, A.A., Kelleher, N.L.: From Protein Complexes to Subunit Backbone Fragments: A Multi-stage Approach to Native Mass Spectrometry. *Anal. Chem.*, **85**, 11163–11173 (2013)

51. Rosati, S., van den Bremer, E.T.J., Schuurman, J., Parren, P., Kamerling, J., Heck, A.J.R.: In-depth qualitative and quantitative analysis of composite glycosylation profiles and other micro-heterogeneity on intact monoclonal antibodies by high-resolution native mass spectrometry using a modified Orbitrap. *MAbs*, **5**, 917–924 (2013)

52. Rosati, S., Thompson, N.J., Barendregt, A., Hendriks, L.J.A., Bakker, A.B.H., de Kruif, J., Throsby, M., van Duijn, E., Heck, A.J.R.: Qualitative and semiquantitative analysis of composite mixtures of antibodies by native mass spectrometry. *Anal. Chem.*, **84**, 7227–7232 (2012)

53. Boldin, I.A., Nikolaev, E.N.: Fourier transform ion cyclotron resonance cell with dynamic harmonization of the electric field in the whole volume by shaping of the excitation and detection electrode assembly. *Rapid Commun. Mass Spectrom.*, **25**, 122–126 (2011)

54. Nikolaev, E.N., Boldin, I.A., Jertz, R., Baykut, G.: Initial Experimental Characterization of a New Ultra-High Resolution FTICR Cell with Dynamic Harmonization. *J. Am. Soc. Mass Spectrom.*, **22**, 1125–1133 (2011)

55. Li, H., Wolff, J.J., van Orden, S.L., Loo, J.A.: Native Top-Down Electrospray Ionization-Mass Spectrometry of 158 kDa Protein Complex by High-Resolution Fourier Transform Ion Cyclotron Resonance Mass Spectrometry. *Anal. Chem.*, **86**, 317–320 (2014)

56. Tolmachev, A.V., Udseth, H.R., Smith, R.D.: Radial stratification of ions as a function of mass to charge ratio in collisional cooling radio frequency multipoles used as ion guides or ion traps. *Rapid Commun. Mass Spectrom.*, **14**, 1907–1913 (2000)

57. Tahallah, N., Pinkse, M., Maier, C.S., Heck, A.J.: The effect of the source pressure on the abundance of ions of noncovalent protein assemblies in an electrospray ionization orthogonal time-of-flight instrument. *Rapid Commun. Mass Spectrom.*, **15**, 596–601 (2001)

58. Lewin, M., Guilhaus, M., Wildgoose, J., Hoyes, J., Bateman, B.: Ion dispersion near parallel wire grids in orthogonal acceleration time-of-flight mass spectrometry: predicting the effect of the approach angle on resolution. *Rapid Commun. Mass Spectrom.*, **16**, 609–615 (2002)

59. Lee, J., Reilly, Peter T. A.: Limitation of Time-of-Flight Resolution in the Ultra High Mass Range. *Anal. Chem.*, **83**, 5831–5833 (2011)

60. Mann, M., Meng, C.K., Fenn, J.B.: Interpreting mass spectra of multiply charged ions. *Anal. Chem.*, **61**, 1702–1708 (1989)

61. Senko, M.W., Beu, S.C., McLafferty, F.W.: Determination of monoisotopic masses and ion populations for large biomolecules from resolved isotopic distributions. *J. Am. Soc. Mass Spectrom.*, **6**, 229–233 (1995)

62. Horn, D.M., Zubarev, R.A., McLafferty, F.W.: Automated reduction and interpretation of high resolution electrospray mass spectra of large molecules. *J. Am. Soc. Mass Spectrom.*, **11**, 320–332 (2000)

63. Kaur, P., O'Connor, P.B.: Algorithms for automatic interpretation of high resolution mass spectra. *J. Am. Soc. Mass Spectrom.*, **17**, 459–468 (2006)

64. Frahm, J.L., Mason, C.J., Muddiman, D.C.: Utility of accurate monoisotopic mass measurements to confidently identify lambda exonuclease generated single-stranded amplicons containing 7-deaza analogs by electrospray ionization FT-ICR mass spectrometry. *Int. J. Mass Spectrom.*, **234**, 79–87 (2004)

65. Zhang, H., Cui, W., Gross, M.L., Blankenship, R.E.: Native mass spectrometry of photosynthetic pigment–protein complexes. *FEBS Lett.*, **587**, 1012–1020 (2013)

66. Lorenzen, K., Versluis, C., van Duijn, E., van den Heuvel, R.H.H., Heck, A.J.R.: Optimizing macromolecular tandem mass spectrometry of large non-covalent complexes using heavy collision gases. *Int. J. Mass Spectrom.*, **268**, 198–206 (2007)

67. Sobott, F., Robinson, C.V.: Characterising electrosprayed biomolecules using tandem-MS—the noncovalent GroEL chaperonin assembly. *Int. J. Mass Spectrom.*, **236**, 25–32 (2004)

68. Benesch, J.L.P.: Collisional activation of protein complexes: picking up the pieces. *J. Am. Soc. Mass Spectrom.*, **20**, 341–348 (2009)

69. Tolić, L.P., Bruce, J.E., Lei, Q.P., Anderson, G.A., Smith, R.D.: In-trap cleanup of proteins from electrospray ionization using soft sustained off-resonance irradiation with Fourier transform ion cyclotron resonance mass spectrometry. *Anal. Chem.*, **70**, 405–408 (1998)

70. Ruotolo, B.T., Hyung, S.-J., Robinson, P.M., Giles, K., Bateman, R.H., Robinson, C.V.: Ion mobility–mass spectrometry reveals long-lived, unfolded intermediates in the dissociation of protein complexes. *Angew. Chem. Int. Ed.*, **46**, 8001–8004 (2007)

71. Sun, N., Soya, N., Kitova, E.N., Klassen, J.S.: Nonspecific interactions between proteins and charged biomolecules in electrospray ionization mass spectrometry. *J. Am. Soc. Mass Spectrom.*, **21**, 472–481 (2010)

72. Freeke, J., Robinson, C.V., Ruotolo, B.T.: Residual counter ions can stabilise a large protein complex in the gas phase. *Int. J. Mass Spectrom.*, **298**, 91–98 (2010)

73. Dyachenko, A., Gruber, R., Shimon, L., Horovitz, A., Sharon, M.: Allosteric mechanisms can be distinguished using structural mass spectrometry. *Proc. Natl. Acad. Sci. U.S.A.*, **110**, 7235–7239 (2013)

74. Smith, A.M., Jahn, T.R., Ashcroft, A.E., Radford, S.E.: Direct observation of oligomeric species formed in the early stages of amyloid fibril formation using electrospray ionisation mass spectrometry. *J. Mol. Biol.*, **364**, 9–19 (2006)

75. Ruotolo, B.T., Benesch, J.L.P., Sandercock, A.M., Hyung, S.-J., Robinson, C.V.: Ion mobility–mass spectrometry analysis of large protein complexes. *Nat. Protoc.*, **3**, 1139–1152 (2008)

76. Kłoniecki, M., Jabłonowska, A., Poznański, J., Langridge, J., Hughes, C., Campuzano, I., Giles, K., Dadlez, M.: Ion mobility separation coupled with MS detects two structural states of Alzheimer's Disease Aβ1–40 peptide oligomers. *J. Mol. Biol.*, **407**, 110–124 (2011)

Figure Legends

Figure 1. Illustrative examples for the varied applicability of native MS in structural biology. **(a)** Topology model of a protein complex. Native ESI-MS spectrum of two major variants of the TtCmr complex, the host defense CRISPR-Cas system of *T. thermophilus*. All in all, nine (sub)complexes of TtCmr were detected and mass analyzed from which a first structural model of the complex could be derived (adapted from [21] with permission of Elsevier, EMDB accession number of the displayed structure: EMD-2418). **(b)** Virus assembly. The intact capsid of bacteriophage HK97 (Prohead I^{gp5}) mass analyzed by native ESI-MS on a QTOF. Charge states are just resolved allowing the molecular weight to be determined to 18 MDa, likely the highest mass ever reported by ESI-MS with charge state resolution (adapted from [22] with permission of John Wiley and Sons, PDB accession number of the structure: 3QPR). **(c)** Protein-lipid complexes. Native MS of the membrane-embedded transporter P-glycoprotein in complex with the anionic phospholipids 1-palmitoyl-2-oleoyl-sn-glycero-3-phosphate (upper panel) and 1-palmitoyl-2-oleoyl-sn-glycero-3-phospho-(1'-rac-glycerol) (lower panel) on a QTOF instrument. Samples were electrosprayed from ammonium acetate buffer, containing 0.02% detergent (n-dodecyl-β-D-maltoside). Peaks are labeled with the numbers of bound phospholipids (adapted from [19] with permission of PNAS, PDB accession number of the structure: 3G5U). **(d)** Protein-carbohydrate complexes. Analysis of pentasaccharide binding (L) to the cholera toxin B subunit homopentamer (CTB5) by QTOF native ESI-MS. Specific binding of three, four or five ligands was detected (adapted from [18] with permission of Springer, PDB accession number of the structure: 3CHB)

Figure 2. Theoretical and experimental mass resolution plotted against *m/z*. R-versus-*m/z* plots for the three mass analyzers (FTICR, Orbitrap and TOF) are based on their respective R_{max} values that have been reported at *m/z* 5,000–6,000 (FTICR: 40,000 (personal communication with Michael L. Gross, Washington University in St. Louis), Orbitrap: 25,000 [33], TOF: 7,000 [30]) and the theoretically achievable relations between analyzer mass resolution and *m/z* (FTICR (black line): $R \sim z/m$, Orbitrap (blue line): $R \sim (z/m)^{0.5}$, TOF (cyan line): R = constant). Dotted lines in the FTICR and Orbitrap graphs represent theoretical values for *m/z* ranges that are (currently) not accessible with these mass analyzers. For all other curves we calculated $(m/z)/(\Delta m/z)$ for molecular weights between 50 Da and 20 MDa. The experimentally derived relationship between the mass of globular proteins and their charging behavior in native MS [22] was used to convert these molecular weights into *m/z* values. To determine R_{max}, as it is limited by the width of the isotope envelope of a native protein (red line), we divided the *m/z* values by $\Delta m/z$ being derived from the width of the isotope distribution that scales with the square root of the molecular weight, as described in detail elsewhere [22]. For R_{min} needed to separate consecutive charge states (green line) we calculated *m/z* and *m/(z+1)*. Finally, the *m/z* values corresponding to $[M+nH]^{n+}$ and $[M+(n-1)H+Na]^{n+}$ were taken into account for the calculation of

R_{min} necessary to separate bare ions from a species bound to one Na^+ (orange line). For both R_{min} calculations, we assumed that a single species would appear as a Gaussian-distributed peak in the mass spectra. With regard to this, we calculated the maximum *Δm/z* that just allows neighboring peaks to be separated at 50% of their height. At *m/z* 3,000–4,000, R_{min} for Na-adduct separation exceeds the maximum resolution that is attainable according to the width of the isotope distribution (orange and red line intersect). Consequently, $[M+nH]^{n+}$ and $[M+(n-1)H+Na]^{n+}$ ions cannot be separated at half-maximum peak height above this value. This is marked by the transition from a continuous to a dotted orange line

Figure 3. Adduct ions affect mass resolving power. Baseline isotope mass resolution does not permit to distinguish between bare, sodium- and ammonium-bound ions of a 150 kDa Averagine protein using native ESI-MS. According to the empirical charging behavior of globular proteins in native MS [22], 26+ is the most abundant charge state for a molecular weight of 150 kDa. Therefore, we simulated the peaks of 26-fold charged cations of 150 kDa Averagine (1,350 Averagine residues [61]) with MassLynx V4.1, assuming baseline isotope mass resolution (R = 500,000). The isotope distributions of unmodified (green), ammonium-bound (orange) and sodium-bound (red) protein ions were simulated individually and subsequently summed up to produce the final mass spectrum (black)

Figure 4. Experimental peaks of globular protein complexes are substantially broader than simulated peaks of their molecular ions. The apparent mass resolution R_{nat} depends on the pre-set maximum mass resolution (R_{max}) and the efficiency of adduct removal. **(a)** Shown are mass spectra of a 71+ charged GroEL ion. These were measured on an Orbitrap (blue) and a QTOF (cyan) instrument, both operating at a maximum instrument mass resolution of R_{max} = 5,000, or simulated with MassLynx V4.1 at R_{max} = 5,000 (red), 10,000 (orange), 20,000 (yellow), 40,000 (green). The black curve represents the natural isotope envelope of GroEL. Numbers in parentheses correspond to the apparent mass resolutions R_{nat}, determined by measuring the experimental peak widths. **(b)** R_{nat} of the simulated mass spectra is plotted against the R_{max} values that were assumed in the respective simulations. The correlation between R_{nat} and R_{max} becomes weaker as R_{nat} approximates the ultimate resolution limit that is given by the width of the isotope envelope (dotted line)

Figure 5. Native ESI-MS analysis of GroEL-ATP. These complexes were electrosprayed from an EDDA buffer using a QTOF instrument. **(a)** Mass spectrum of the 58+ charge state of GroEL. After incubation of intact GroEL with 5 µM ATP, peaks corresponding to different numbers of bound ATP molecules are detected. **(b)** The deconvoluted spectrum, assuming binding of 0–4 ATP molecules to GroEL, is in good agreement with the experimental data (adapted from reference [73] with permission of PNAS)

Figure 6. Incomplete desolvation may lead to shifts in *m/z* and (co-)isolation of unwanted precursor ions in tandem MS. In-source activation of HK97 capsomers prevents co-isolation of adjacent species in tandem MS experiments. Spectra were recorded with different settings for in-source activation (ISA, prior to precursor ion selection) and activation in the collision cell (CCA, after precursor ion selection). The *m/z* selected for MSMS is indicated with a dotted line. **(a)** MS spectrum of capsomers at high activation in the collision cell. **(b)** MSMS spectrum at minimal collisional activation. **(c)** MSMS spectrum at high activation in the collision cell without in-source activation. **(d)** MSMS spectrum at high in-source activation and minimal activation in the collision cell

Figure 7. Hyphenation of ion mobility and mass spectrometry may enhance mass resolving power in native MS. Separation of Aβ oligomers by means of IMMS. The species present in the *m/z*-versus-drift time plot are indicated as colored spots, with the intensity increasing from purple to yellow. Insets in the left panel show mass spectra of the respective oligomeric states of Aβ being populated at different drift times (adapted from reference [76] with permission of Elsevier)

Figure 1

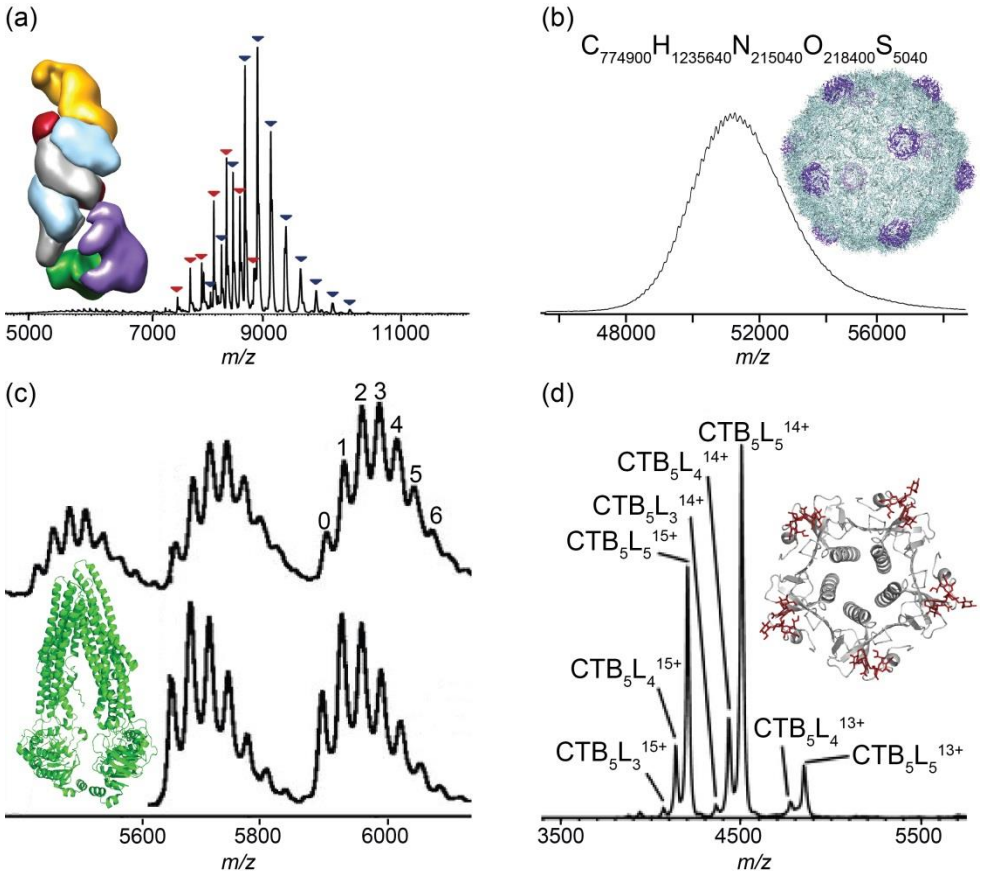
(a)
5000
7000
9000
11000
m/z
(b)
C774900H1235640N215040O218400S5040
48000
52000
56000
m/z
(c)
0
1
2 3
4
5
6
5600
5800
6000
m/z
(d)
CTB5L5 14+
CTB5L4 14+
CTB5L3 14+
CTB5L5 15+
CTB5L4 15+
CTB5L3 15+
CTB5L4 13+
CTB5L5 13+
3500
4500
5500
m/z

Figure 2

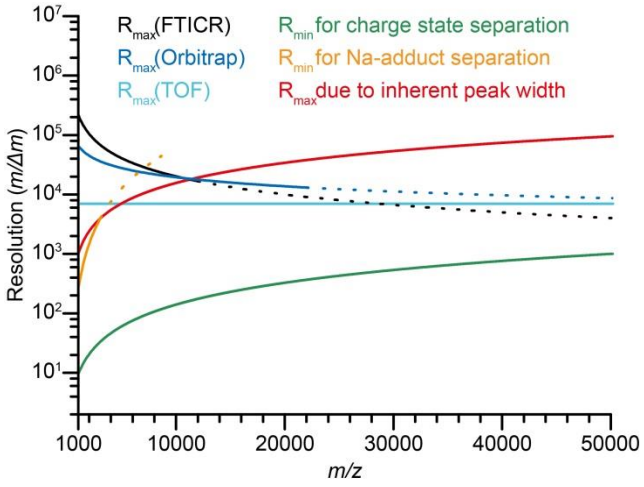
R_{max}(FTICR)
R_{max}(Orbitrap)
R_{max}(TOF)
R_{min} for charge state separation
R_{min} for Na-adduct separation
R_{max} due to inherent peak width
Resolution (m/Δm)
10^7
10^6
10^5
10^4
10^3
10^2
10^1
1000
10000
20000
30000
40000
50000
m/z

Figure 3

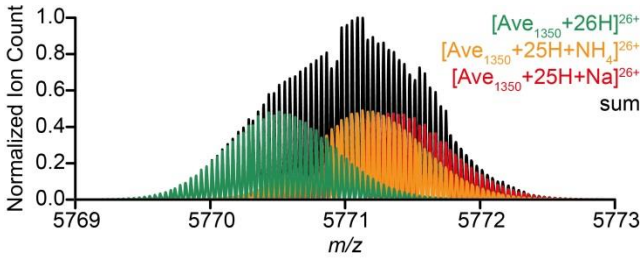
Normalized Ion Count
1.0
0.8
0.6
0.4
0.2
0.0
5769
5770
5771
5772
5773
m/z
[Ave1350+26H]26+
[Ave1350+25H+NH4]26+
[Ave1350+25H+Na]26+
sum

Figure 4

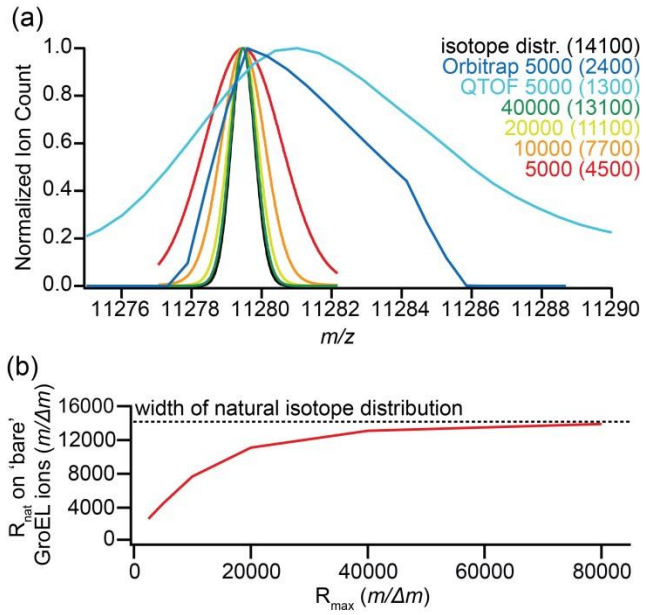
(a)
Normalized Ion Count
1.0
0.8
0.6
0.4
0.2
0.0
11276 11278 11280 11282 11284 11286 11288 11290
m/z
isotope distr. (14100)
Orbitrap 5000 (2400)
QTOF 5000 (1300)
40000 (13100)
20000 (11100)
10000 (7700)
5000 (4500)
(b)
R_nat on 'bare' GroEL ions (m/Δm)
16000
12000
8000
4000
0
width of natural isotope distribution
0
20000
40000
60000
80000
R_max (m/Δm)

Figure 5

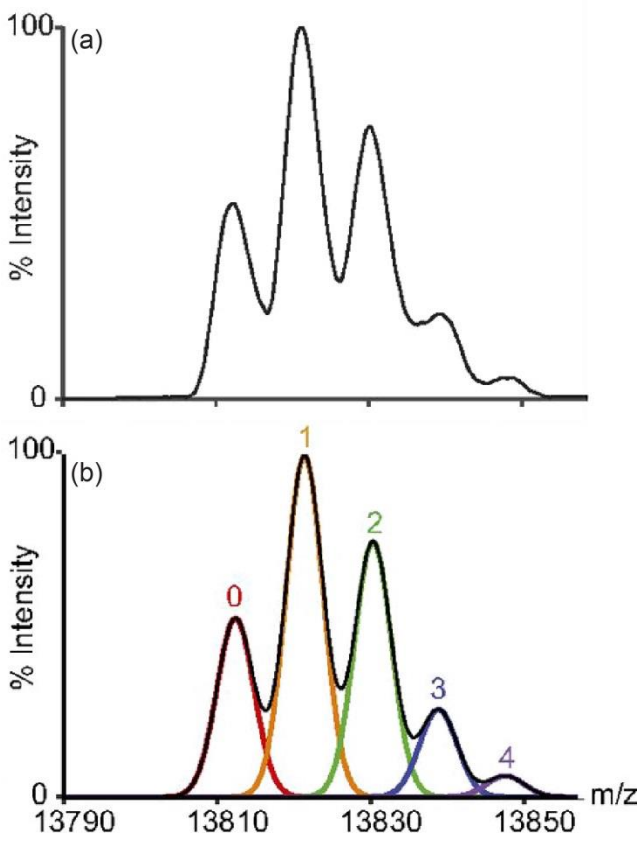
100
(a)
% Intensity
0
100
(b)
% Intensity
0
1
2
0
3
4
m/z
13790
13810
13830
13850

Figure 6

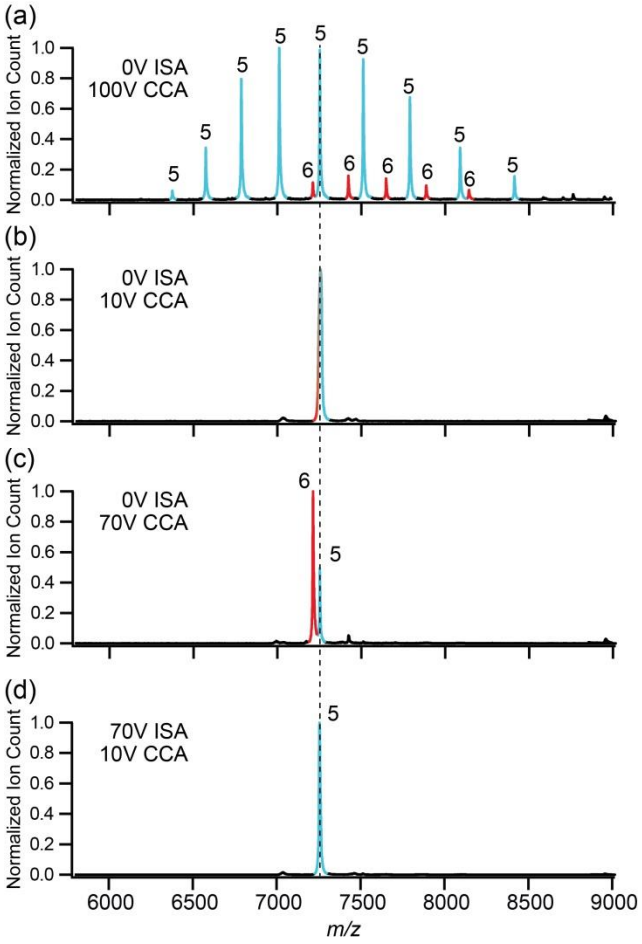
(a)
0V ISA
100V CCA
(b)
0V ISA
10V CCA
(c)
0V ISA
70V CCA
(d)
70V ISA
10V CCA
Normalized Ion Count
m/z
6000
6500
7000
7500
8000
8500
9000

Figure 7

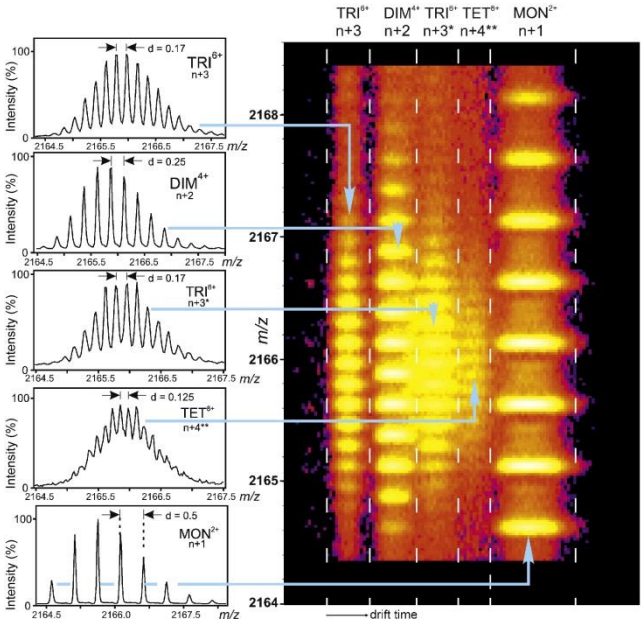
TRI6+ n+3
DIM4+ n+2
TRI6+ n+3*
TET6+ n+4**
MON2+ n+1
d = 0.17
TRI6+ n+3
d = 0.25
DIM4+ n+2
d = 0.17
TRI6+ n+3*
d = 0.125
TET6+ n+4**
d = 0.5
MON2+ n+1
Intensity (%)
m/z
2168
2167
2166
2165
2164
drift time